

Towards Automatic Neural Architecture Search within General Super-Networks

Tianyi Chen, Luming Liang, Tianyu Ding, Ilya Zharkov

Microsoft, Redmond, WA 98052, USA

{tiachen, lulian, tianyuding, zharkov}@microsoft.com

Abstract

Existing neural architecture search (NAS) methods typically rely on pre-specified super deep neural networks (super-networks) with handcrafted search spaces beforehand. Such requirements make it challenging to extend them onto general scenarios without significant human expertise and manual intervention. To overcome the limitations, we propose the third generation of Only-Train-Once (OTOv3). OTOv3 is perhaps the first automated system that trains general super-networks and produces high-performing sub-networks in the one shot manner without pre-training and fine-tuning. Technologically, OTOv3 delivers three noticeable contributions to minimize human efforts: (i) automatic search space construction for general super-networks; (ii) a Hierarchical Half-Space Projected Gradient (H2SPG) that leverages the dependency graph to ensure the network validity during optimization and reliably produces a solution with both high performance and hierarchical group sparsity; and (iii) automatic sub-network construction based on the super-network and the H2SPG solution. Numerically, we demonstrate the effectiveness of OTOv3 on a variety of super-networks, including RegNet, StackedUnets, SuperResNet, and DARTS, over benchmark datasets such as CIFAR10, Fashion-MNIST, ImageNet, STL-10, and SVNH. The sub-networks computed by OTOv3 achieve competitive even superior performance compared to the super-networks and other state-of-the-arts. The library will be released at https://github.com/tianyic/only_train_once.

1 Introduction

Deep neural networks (DNNs) have achieved remarkable success in various fields, which success is highly dependent on their sophisticated underlying architectures (LeCun et al., 2015; Goodfellow et al., 2016). To design effective DNN architectures, human expertise have handcrafted numerous popular DNNs such as ResNet (He et al., 2016) and transformer (Vaswani et al., 2017). However, such human efforts may not be scalable enough to meet the increasing demands for customizing DNNs for diverse tasks. To address this issue, Neural Architecture Search (NAS) has emerged to automate the network creations and reduce the need for human expertise (Elsken et al., 2018).

Among current NAS studies, gradient-based methods (Liu et al., 2018; Yang et al., 2020; Xu et al., 2019; Chen et al., 2021b) are perhaps the most popular because of their efficiency. Such methods build an over-parameterized super-network covering all candidate connections and operations, parameterize operations via introducing auxiliary architecture variables with weight sharing, then search a (sub)optimal sub-network via formulating and solving a multi-level optimization problem.

Despite the advancements in gradient-based methods, their usage is still limited due to certain inconvenience. In particular, their automation relies on manually determining the search space for a pre-specified super-network beforehand, and requires the manual introduction of auxiliary architecture variables onto the prescribed search space. To extend these methods onto other super-networks, the

users still need to manually construct the search pool, then incorporate the auxiliary architecture variables along with building the whole complicated multi-level optimization training pipeline. The whole process necessitates significant domain-knowledge and engineering efforts, thereby being inconvenient and time-consuming for users. Therefore, it is natural to ask whether we could reach an

Objective. *Given a general super-network, automatically generate its search space, train it once, and construct a sub-network that achieves a dramatically compact architecture and high performance.*

Achieving the objective is severely challenging in terms of both engineering developments and algorithmic designs, consequently not achieved yet by the existing NAS works to the best of our knowledge. However, the objective has been recently achieved in an analogous task so-called structured pruning (Lin et al., 2019) by the second generation of Only-Train-Once framework (OTOv2) (Chen et al., 2021a, 2023). From the perspective of computational graph, the standard NAS could be considered as removing entire redundant connections (cutting edges) and operations (vertices) from super-networks. Structured pruning can be largely interpreted as a complementary NAS that removes the redundancy inside each vertex (slims operations) but preserves all the connections. OTOv2 first achieves the objective in the view of structured pruning that given a general DNN, automatically trains it only once to achieve both high performance and a slimmer model architecture without pre-training and fine-tuning.

	OTOv3	OTOv2	Other NAS
General DNNs	✓	✓	✗
Autonomy	✓	✓	✗
Remove Connections	✓	✗	✓
Remove Operations	✓	✗	✓
Slim Operations	✓ [†]	✓	✗

[†] Support while is not the focus and discussed in this work.

We now build the third-generation of Only-Train-Once (OTOv3) that reaches the objective from the perspective of the standard NAS. OTOv3 automatically generates a search space given a general super-network, trains and identifies redundant connections and vertices, then builds a sub-network that achieves both high performance and compactness. As the library usage presented aside, the whole procedure can be automatically proceeded, dramatically reduce the human efforts, and fit for general super-networks and applications. Our main contributions can be summarized as follows.

OTOv3 Library Usage

```

1 from only_train_once import OTO
2 # General Super-Network
3 oto = OTO(super_net, cut_edges=True)
4 optimizer = oto.h2spg()
5 # Train as normal
6 optimizer.step()
7 oto.construct_subnet(cut_edges=True)

```

- **Infrastructure for Automated General Super-Network Training and Sub-Network Searching.** We propose OTOv3 that perhaps the first automatically trains and searches within a general super-network to deliver a compact sub-network by erasing redundant connections and operations in the one-shot manner. As the previous OTO versions, OTOv3 trains the super-network only once without the need of pre-training and fine-tuning and is pluggable into various deep learning applications.
- **Automated Search Space Generation.** We propose a novel graph algorithm to automatically explore and establish a dependency graph given a general super-network, then analyze the dependency to form a search space consisting of minimal removal structures. The corresponding trainable variables are then partitioned into so-called generalized zero-invariant groups (GeZIGs).
- **Hierarchical Half-Space Projected Gradient (H2SPG).** We propose a novel H2SPG optimizer that perhaps the first solves a hierarchical structured sparsity problem for general DNNs. H2SPG computes a solution x_{H2SPG}^* of both high performance and desired hierarchical group sparsity in the manner of GeZIGs. Compared to other optimizers, H2SPG considers the hierarchy of dependency graph to produce sparsity for ensuring the validness of the subsequent sub-network.
- **Automated Sub-Network Construction.** We propose a novel graph algorithm to automatically construct a sub-network upon the super-network parameterized as x_{H2SPG}^* . The resulting sub-network returns the exact same outputs as the super-network thereby no need of further fine-tuning.
- **Experimental Results.** We demonstrate the effectiveness of OTOv3 on extensive super-networks including StackedUnets, SuperResNet and DARTS, over benchmark datasets including CIFAR10, Fashion-MNIST, ImageNet, STL-10, and SVNH. OTOv3 is the first framework that could automatically deliver compact sub-networks upon general super-networks to the best of our knowledge. Meanwhile the sub-networks exhibit competitive even superior performance to the super-networks.

2 Related Work

Neural Architecture Search (NAS). Early NAS works utilized reinforcement learning and evolution techniques to search for high-quality architectures (Zoph & Le, 2016; Pham et al., 2018; Zoph

et al., 2018), while they were computationally expensive. Later on, differentiable (gradient-based) methods were introduced to accelerate the search process. These methods start with a super-network covering all possible connection and operation candidates, and parameterize them with auxiliary architecture variables. They establish a multi-level optimization problem that alternatingly updates the architecture and network variables until convergence (Liu et al., 2018; Chen et al., 2019; Xu et al., 2019; Yang et al., 2020; Hosseini & Xie, 2022). However, these methods require a significant amount of **handcraftiness** from users in advance to **manually** establish the search space, introduce additional architecture variables, and build the multi-level training pipeline. The sub-network construction is also network-specific and not flexible. All requirements necessitate remarkable domain-knowledge and expertise, making it difficult to extend to general super-networks and broader scenarios.

Automated Structured Pruning for General DNNs. Structure pruning is an orthogonal but related paradigm to standard NAS. Rather than removing entire operations and connections, it focuses on slimming individual vertices (Han et al., 2015; Chen et al., 2020). Similarly, prior structure pruning methods required numerous handcraftiness and domain knowledge, which limited their broader applicability. However, recent methods such as OTOv2 (Chen et al., 2023) and DepGraph (Fang et al., 2023) have made progress in automating the structure pruning for general DNNs. OTOv2 is a one-shot method that does not require pre-training or fine-tuning. DepGraph involves a multi-stage training pipeline that requires some post-training efforts. In this work, we propose the third-generation version of OTO that enables automatic sub-network searching and training for general super-networks.

Hierarchical Structured Sparsity Optimization. We formulate the underlying optimization problem of OTOv3 as a hierarchical structured sparsity problem. Its solution possesses high group sparsity indicating redundant structures and obeys specified hierarchy. There exist deterministic optimizers solving such problems via introducing latent variables (Zhao et al., 2009), while are impractical for stochastic DNN tasks. Meanwhile, stochastic optimizers rarely study such problem. In fact, popular stochastic sparse optimizers such as HSPG (Chen et al., 2021a), AdaHSPG+ (Dai et al., 2023), DHSPG (Chen et al., 2023), proximal methods (Xiao & Zhang, 2014) and ADMM (Lin et al., 2019) overlook the hierarchy constraint. Employing them into OTOv3 typically delivers invalid sub-networks. We propose H2SPG that considers graph dependency to solve it for general DNNs.

3 OTOv3

OTOv3 is an automated one-shot system that trains a general super-network and constructs a sub-network. The produced sub-network is not only high-performing but also has a dramatically compact architecture that is suitable for various shipping environments. The entire process minimizes the need for human efforts and is suitable for general DNNs. As outlined in Algorithm 1, given a general super-network \mathcal{M} , OTOv3 first explores and establishes a dependency graph. Upon the dependency graph, a search space is automatically constructed and corresponding trainable variables are partitioned into generalized zero-invariant groups (GeZIGs) (Section 3.1). A hierarchical structured sparsity optimization problem is then formulated and solved by a novel Hierarchical Half-Space Projected Gradient (H2SPG) (Section 3.2). H2SPG considers the hierarchy inside the dependency graph and computes a solution $\mathbf{x}_{\text{H2SPG}}^*$ of both high-performance and desired hierarchical group sparsity over GeZIGs. A compact sub-network \mathcal{M}^* is finally constructed via removing the structures corresponding to the identified redundant GeZIGs and their dependent structures (Section 3.3). \mathcal{M}^* returns the exact same output as the super-network parameterized as $\mathbf{x}_{\text{H2SPG}}^*$, eliminating the need of fine-tuning.

Algorithm 1 Outline of OTOv3.

- 1: **Input:** A general DNN \mathcal{M} as super-network to be trained and searched (no need to be pretrained).
 - 2: **Automated Search Space Construction.** Establish dependency graph and partition the trainable parameters of \mathcal{M} into generalized zero-invariant groups $\mathcal{G}_{\text{GeZIG}}$ and the complementary $\mathcal{G}_{\text{GeZIG}}^C$.
 - 3: **Train by H2SPG.** Seek a high-performing solution $\mathbf{x}_{\text{H2SPG}}^*$ with hierarchical group sparsity.
 - 4: **Automated Sub-Network \mathcal{M}^* Construction.** Construct a sub-network upon $\mathbf{x}_{\text{H2SPG}}^*$.
 - 5: **Output:** Constructed sub-network \mathcal{M}^* (no need to be fine-tuned).
-

3.1 Automated Search Space Construction

The foremost step is to automatically construct the search space for a general super-network. However, this process presents significant challenges in terms of both engineering developments and algorithmic

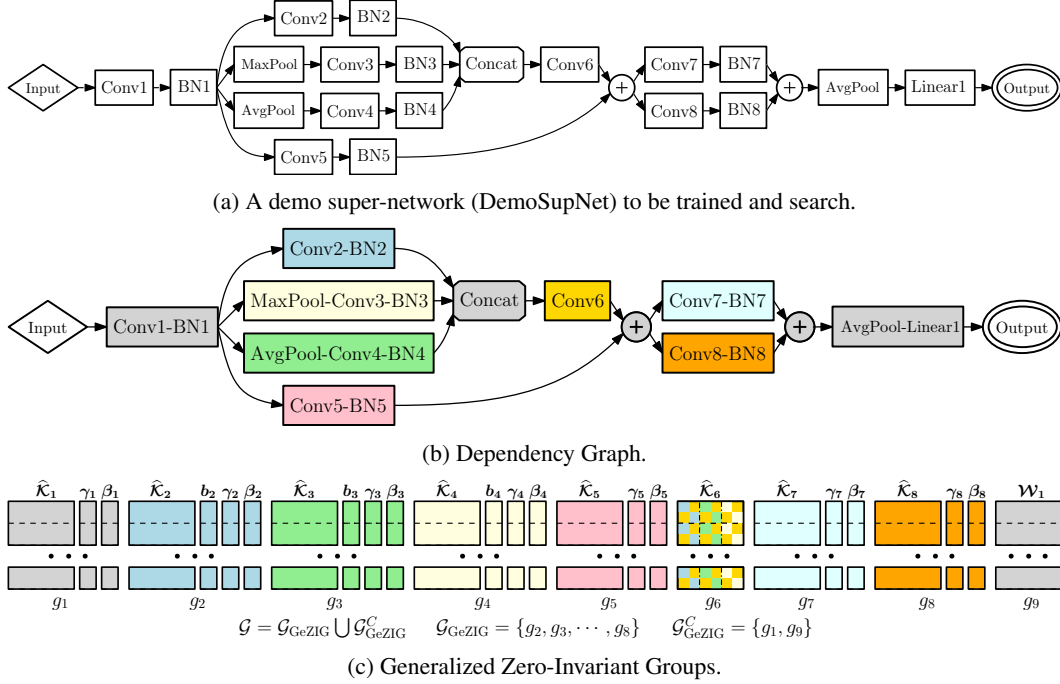


Figure 1: Automated Search Space Construction. $\hat{\mathcal{K}}_i$ and b_i are the flatten filter matrix and bias vector for Conv- i , respectively. γ_i and β_i are the weight and bias vectors for BN- i . \mathcal{W}_i is the weight matrix for Linear- i . The columns of $\hat{\mathcal{K}}_6$ are marked in accordance to its incoming segments.

designs due to the complexity of DNN architecture and the lack of sufficient public APIs. To overcome these challenges, we propose a concept called generalized zero-invariant group (GeZIG) and formulate the search space construction as the GeZIG partition. We have also developed a dedicated graph algorithm to automatically conduct the GeZIG partition for general super-networks.

Generalized Zero-Invariant Group (GeZIG). The key of search space construction is to figure out the structures that can be removed from the super-network. Because of diverse roles of operations and their complicated connections inside a DNN, removing an arbitrary structure may cause the remaining DNN invalid. We say a structure *removal* if and only if the DNN after removing it is still valid. A removal structure is further said *minimal* if and only if it does not contain multiple removal structures. Zero-Invariant Group (ZIG) is proposed in (Chen et al., 2021a, 2023) that describes a class of minimal removal structures satisfying a *zero-invariant property*, i.e., if all variables in ZIG equal to zero, then no matter what the input is, the output is always as zero. ZIG depicts the minimal removal structure *inside each operation* and is the key for realizing automatic one-shot structured pruning. We generalize ZIG as GeZIG that describes a class of minimal removal structures satisfying the zero-invariant property but *consists of entire operations*. More illustrations regarding ZIG versus GeZIG are present in Appendix. For simplicity, throughout the paper, the minimal removal structure is referred to the counterpart consisting of operations in entirety. Consequently, automated search space construction becomes how to automatically explore the GeZIG partition for general DNNs.

Automated GeZIG Partition. As specified in Algorithm 2, automated GeZIG partition involves two main stages. The first stage explores the super-network \mathcal{M} and establishes a dependency graph $(\mathcal{V}_d, \mathcal{E}_d)$. The second stage leverages the affiliations inside the dependency graph to find out minimal removal structures, then partitions their trainable variables to form GeZIGs. For intuitive illustrations, we elaborate the algorithm through a small but complex demo super-network depicted in Figure 1a.

Dependency Graph Construction. Given a super-network \mathcal{M} , we first construct its trace graph $(\mathcal{V}, \mathcal{E})$ displayed as Figure 1a (line 3 in Algorithm 2), where \mathcal{V} represents the set of vertices (operations) and \mathcal{E} represents the connections among them. As OTov2 (Chen et al., 2023), we categorize the vertices into stem vertices, joint vertices, accessory vertices, and unknown vertices. Stem vertices refer to the operations that contain trainable variables and can transform the input tensors into different shapes, e.g., Conv and Linear. The accessory vertices are the operations that may not have trainable

Algorithm 2 Automated Search Space Construction.

- 1: **Input:** A super-network \mathcal{M} to be trained and searched.
 - 2: **Dependency graph construction.**
 - 3: Construct the trace graph $(\mathcal{E}, \mathcal{V})$ of \mathcal{M} .
 - 4: Initialize an empty graph $(\mathcal{V}_d, \mathcal{E}_d)$.
 - 5: Initialize queue $\mathcal{Q} \leftarrow \{\mathcal{S}(v) : v \in \mathcal{V} \text{ is adjacent to the input of trace graph}\}$.
 - 6: **while** $\mathcal{Q} \neq \emptyset$ **do**
 - 7: Dequeue the head segment \mathcal{S} from \mathcal{Q} .
 - 8: Grow \mathcal{S} in the depth-first manner till meet either joint vertex or multi-outgoing vertex \hat{v} .
 - 9: Add segments into \mathcal{V}_d and connections into \mathcal{E}_d .
 - 10: Enqueue new segments into the tail of \mathcal{Q} if \hat{v} has outgoing vertices.
 - 11: **Find minimal removal structures.**
 - 12: Get the incoming vertices $\hat{\mathcal{V}}$ for joint vertices in the $(\mathcal{V}_d, \mathcal{E}_d)$.
 - 13: Group the trainable variables in the vertex $v \in \hat{\mathcal{V}}$ as g_v .
 - 14: Form $\mathcal{G}_{\text{GeZIG}}$ as the union of the above groups, *i.e.*, $\mathcal{G}_{\text{GeZIG}} \leftarrow \{g_v : v \in \hat{\mathcal{V}}\}$.
 - 15: Form $\mathcal{G}_{\text{GeZIG}}^C$ as the union of the trainable variables in the remaining vertices.
 - 16: **Return** trainable variable partition $\mathcal{G} = \mathcal{G}_{\text{GeZIG}} \cup \mathcal{G}_{\text{GeZIG}}^C$ and dynamic dependency graph $(\mathcal{V}_d, \mathcal{E}_d)$.
-

variables and have an single input, *e.g.*, BN and ReLU. Joint vertices aggregate multiple inputs into a single output, *e.g.*, Add and Concat. The remaining vertices are considered as unknown.

We begin by analyzing the trace graph $(\mathcal{V}, \mathcal{E})$ to create a dependency graph $(\mathcal{V}_d, \mathcal{E}_d)$, wherein each vertex in \mathcal{V}_d serves as a potential minimal removal structure candidate. To proceed, we use a queue container \mathcal{Q} to track the candidates (line 5 of Algorithm 2). The initial elements of this queue are the vertices that are directly adjacent to the input of \mathcal{M} , such as Conv1. We then traverse the graph in the breadth-first manner, iteratively growing each element (segment) \mathcal{S} in the queue until a valid minimal removal structure candidate is formed. The growth of each candidate follows the depth-first search to recursively expand \mathcal{S} until the current vertices are considered as endpoints. The endpoint vertex is determined by whether it is a joint vertex or has multiple outgoing vertices, as indicated in line 8 of Algorithm 2. Intuitively, a joint vertex has multiple inputs, which means that the DNN may be still valid after removing the current segment. This suggests that the current segment may be removable. On the other hand, a vertex with multiple outgoing neighbors implies that removing the current segment may cause some of its children to miss the input tensor. For instance, removing Conv1-BN1 would cause Conv2, MaxPool and AvgPool to become invalid due to the absence of input in Figure 1a. Therefore, it is risky to remove such candidates. Once the segment \mathcal{S} has been grown, new candidates are initialized as the outgoing vertices of the endpoint and added into the container \mathcal{Q} (line 10 in Algorithm 2). Such procedure is repeated until the end of graph traversal. Ultimately, a dependency graph $(\mathcal{V}_d, \mathcal{E}_d)$ is created, as illustrated in Figure 1b.

Form GeZIGs. We proceed to identify the minimal removal structures in $(\mathcal{V}_d, \mathcal{E}_d)$ to create the GeZIG partition. The qualified instances are the vertices in \mathcal{V}_d that have trainable variables and all of their outgoing vertices are joint vertices. This is because a joint vertex has multiple inputs and remains valid even after removing some of its incoming structures, as indicated in line 12 in Algorithm 2. Consequently, their trainable variables are grouped together into GeZIGs (line 13-14 in Algorithm 2 and Figure 1c). The remaining vertices are considered as either unremovable or belonging to a large removal structure, which trainable variables are grouped into the $\mathcal{G}_{\text{GeZIG}}^C$ (the complementary to $\mathcal{G}_{\text{GeZIG}}$). As a result, for the super-network \mathcal{M} , all its trainable variables are encompassed by the union $\mathcal{G} = \mathcal{G}_{\text{GeZIG}} \cup \mathcal{G}_{\text{GeZIG}}^C$, and the corresponding structures in $\mathcal{G}_{\text{GeZIG}}$ constitute its search space.

3.2 Hierarchical Half-Space Projected Gradient (H2SPG)

Given a super-network \mathcal{M} and its group partition $\mathcal{G} = \mathcal{G}_{\text{GeZIG}} \cup \mathcal{G}_{\text{GeZIG}}^C$, the next is to jointly search for a valid sub-network \mathcal{M}^* that exhibits the most significant performance and train it to high performance. Searching a sub-network is equivalent to identifying the redundant structures in $\mathcal{G}_{\text{GeZIG}}$ to be further removed and ensures the remaining network still valid. Training the sub-network becomes optimizing over the remaining groups in \mathcal{G} to achieve high performance. We formulate a hierarchical structured sparsity problem to accomplish both tasks simultaneously as follows.

$$\underset{\mathbf{x} \in \mathbb{R}^n}{\text{minimize}} f(\mathbf{x}), \text{ s.t. } \text{Cardinality}(\mathcal{G}^0) = K, \text{ and } (\mathcal{V}_d/\mathcal{V}_{\mathcal{G}^0}, \mathcal{E}_d/\mathcal{E}_{\mathcal{G}^0}) \text{ is valid}, \quad (1)$$

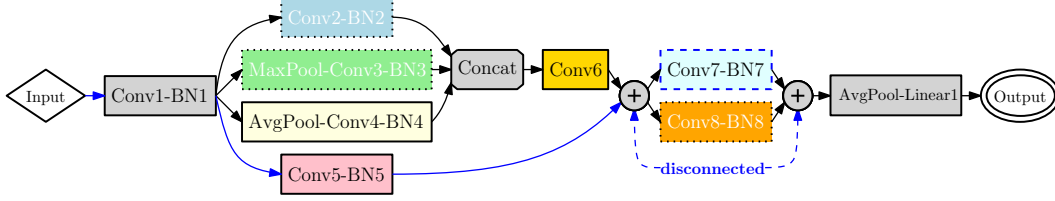


Figure 2: Check validness of redundant candidates. Target group sparsity $K = 3$. Conv7-BN7 has larger redundancy score than Conv2-BN2. Dotted vertices are marked as redundant candidates.

where f is the prescribed loss function, $\mathcal{G}^0 := \{g \in \mathcal{G}_{\text{GeZIG}} | [x]_g = 0\}$ is the set of zero groups in $\mathcal{G}_{\text{GeZIG}}$, which cardinality measures its size. K is the target group sparsity, indicating the number of GeZIGs that should be identified as redundant. The redundant GeZIGs are projected onto zero, while the important groups are preserved as non-zero and optimized for high performance. A larger K dictates a higher sparsity level that produces a more compact sub-network with fewer FLOPs and parameters. $(\mathcal{V}_d/\mathcal{V}_{\mathcal{G}^0}, \mathcal{E}_d/\mathcal{E}_{\mathcal{G}^0})$ refers to the graph removing vertices and edges corresponding to zero groups \mathcal{G}^0 . This graph being valid is specified for NAS that requires the zero groups distributed obeying the hierarchy of super-network to ensure the resulting sub-network functions correctly.

Problem (1) is difficult to solve due to the non-differential and non-convex sparsity constraint and the graph validity constraint. Existing optimizers such as DHSPG (Chen et al., 2023) overlook the architecture evolution and hierarchy during the sparsity exploration, which is crucial to (1). In fact, they are mainly applied for pruning tasks, where the connections and operations are preserved (but become slimmer). Consequently, employing them onto (1) usually produces invalid sub-networks.

Outline of H2SPG. To effectively solve problem (1), we propose a novel H2SPG to consider the hierarchy and ensure the validness of graph architecture after removing redundant vertices and connections during the optimization process. To the best of our knowledge, H2SPG is the first the optimizer that successfully solves such hierarchical structured sparsity problem (1), which outline is stated in Algorithm 3.

H2SPG is built upon the DHSPG in OTOv2 but with dedicated designs regarding the hierarchical constraint. In general, H2SPG is a hybrid multi-phase optimizer that first partitions the groups of variables into important and potentially redundant segments, then employs specified updating mechanisms onto different segments to achieve a solution with both desired hierarchical group sparsity and high performance. The variable partition considers the hierarchy of dependency graph $(\mathcal{V}_d, \mathcal{E}_d)$ to ensure the validness of the resulting sub-network graph. Vanilla stochastic gradient descent (SGD) or its variant such as Adam (Kingma & Ba, 2014) optimizes the important variables to achieve the high performance. Half-space gradient descent (Chen et al., 2021a) identifies redundant groups among the candidates and projects them onto zero without sacrificing the objective function to the largest extent.

Warm-Up Phase. To proceed, H2SPG first warms up all variables by conducting SGD or its variants T_w steps (line 4-5 in Algorithm 3). During each warm-up step t , a redundancy score of each group $g \in \mathcal{G}_{\text{GeZIG}}$ is computed upon the current iterate \mathbf{x}_t and exponentially averaged by a momentum coefficient ω (line 6-7 in Algorithm 3). Larger redundancy score indicates the group exhibits less prediction power, thus may be redundant. The redundancy score calculation is modular, where we follow DHSPG to consider the cosine similarity between negative gradient $-\nabla f(\mathbf{x}_t)_g$ and the projection direction $-\mathbf{x}_g$ as well as the average variable magnitude. After warm-up, the redundancy

Algorithm 3 Hierarchical Half-Space Projected Gradient

- 1: **Input:** initial variable $\mathbf{x}_0 \in \mathbb{R}^n$, initial learning rate α_0 , warm-up steps T_w , target group sparsity K , momentum ω , dependency graph $(\mathcal{V}_d, \mathcal{E}_d)$ and group partitions \mathcal{G} .
 - 2: **Warm-up Phase.**
 - 3: **for** $t = 0, 1, \dots, T_w - 1$ **do**
 - 4: Calculate gradient estimate $\nabla f(\mathbf{x}_t)$ or its variant.
 - 5: Update next iterate $\mathbf{x}_{t+1} \leftarrow \mathbf{x}_t - \alpha_t \nabla f(\mathbf{x}_t)$.
 - 6: Calculate redundancy score $s_{t,g}$ for $g \in \mathcal{G}_{\text{GeZIG}}$.
 - 7: Update $s_g \leftarrow \omega s_g + (1 - \omega) s_{t,g}$ for $g \in \mathcal{G}_{\text{GeZIG}}$.
 - 8: Construct \mathcal{G}_r and \mathcal{G}_r^C given scores, \mathcal{G} , $(\mathcal{V}_d, \mathcal{E}_d)$, and K .
 - 9: **Hybrid Training Phase.**
 - 10: **for** $t = T_w, T_w + 1, \dots$, **do**
 - 11: Compute gradient estimate $\nabla f(\mathbf{x}_t)$ or its variant.
 - 12: Update $[\mathbf{x}_{t+1}]_{\mathcal{G}_r^C}$ as $[\mathbf{x}_t - \alpha_t \nabla f(\mathbf{x}_t)]_{\mathcal{G}_r^C}$.
 - 13: Select proper λ_g for each $g \in \mathcal{G}_r$.
 - 14: Compute $[\tilde{\mathbf{x}}_{t+1}]_{\mathcal{G}_r}$ via subgradient descent of ψ .
 - 15: Perform Half-Space projection over $[\tilde{\mathbf{x}}_{t+1}]_{\mathcal{G}_r}$.
 - 16: Update $[\mathbf{x}_{t+1}]_{\mathcal{G}_r} \leftarrow [\tilde{\mathbf{x}}_{t+1}]_{\mathcal{G}_r}$.
 - 17: **Return** the final iterate $\mathbf{x}_{\text{DHSPG}^+}^*$.
-

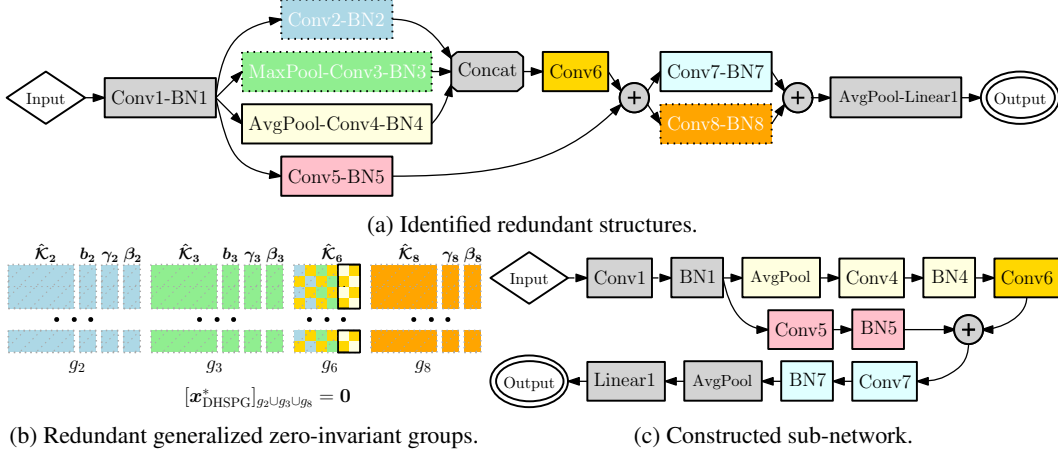


Figure 3: Redundant removal structures identifications and sub-network construction.

scores of all groups in $\mathcal{G}_{\text{GeZIG}}$ are sorted. We then perform a sanity check and select the groups with top-K redundancy scores as the redundant group candidates $\mathcal{G}_r \subseteq \mathcal{G}_{\text{GeZIG}}$. The complementary groups with lower redundancy scores are marked as important ones and form $\mathcal{G}_r^C := \mathcal{G}/\mathcal{G}_r$. The sanity check verifies whether the remaining graph is still connected after removing a vertex. If so, the current vertex is added into \mathcal{G}_r ; otherwise, the subsequent vertex is turned into considerations. As illustrated in Figure 2, though Conv7-BN7 has a larger redundancy score than Conv2-BN2, Conv2-BN2 is marked as potentially redundant but not Conv7-BN7 since there is no path connecting the input and the output of the graph after removing Conv7-BN7. This mechanism largely guarantees that even if all redundant candidates are erased, the resulting sub-network is still functioning as normal.

Hybrid Training Phase. H2SPG then engages into the hybrid training phase to produce desired group sparsity over \mathcal{G}_r and optimize over \mathcal{G}_r^C for pursuing excellent performance till the convergence. This phase mainly follows DHSPG (Chen et al., 2023), and we briefly describe the steps for completeness. In general, for the important groups of variables in \mathcal{G}_r^C , the vanilla SGD or its variant is employed to minimize the objective function to the largest extent (line 11-12 in Algorithm 3). For redundant group candidates in \mathcal{G}_r , we formulate a relaxed non-constrained subproblem as (2) to gradually reduce the magnitudes without deteriorating the objective and project groups onto zeros only if the projection serves as a descent direction for the objective during the training process (line 13-16 in Algorithm 3).

$$\underset{[\mathbf{x}]_{\mathcal{G}_r}}{\text{minimize}} \psi([\mathbf{x}]_{\mathcal{G}_r}) := f([\mathbf{x}]_{\mathcal{G}_r}) + \sum_{g \in \mathcal{G}_r} \lambda_g \|\mathbf{x}_g\|_2, \quad (2)$$

where λ_g is a group-specific regularization coefficient and dedicatedly selected as DHSPG. H2SPG then performs a subgradient descent of ψ over $[\mathbf{x}]_{\mathcal{G}_r}$, followed by a Half-Space projection (Chen et al., 2021a) to effectively produce group sparsity with the minimal sacrifice of the objective function. At the end, a high-performing solution $\mathbf{x}_{\text{H2SPG}}^*$ with desired hierarchical group sparsity is returned.

3.3 Automated Sub-Network Construction.

We finally construct a sub-network \mathcal{M}^* upon the super-network \mathcal{M} and the solution $\mathbf{x}_{\text{H2SPG}}^*$ by H2SPG. The solution $\mathbf{x}_{\text{H2SPG}}^*$ should attain desired target hierarchical group sparsity level and achieve high performance. As illustrated in Figure 3, we first traverse the graph to remove the entire vertices and the related edges from \mathcal{M} corresponding to the redundant GeZIGs being zero, e.g., Conv2-BN2, MaxPool-Conv3-BN3 and Conv8-BN8 are removed due to $[\mathbf{x}_{\text{H2SPG}}^*]_{g_2 \cup g_3 \cup g_8} = \mathbf{0}$. Then, we traverse the graph in the second pass to remove the affiliated structures that are dependent on the removed vertices to keep the remaining operations valid, e.g., the first and second columns in $\hat{\mathcal{K}}_6$ are erased since its incoming vertices Conv2-BN2 and MaxPool-Conv3-BN3 has been removed (see Figure 3b). Next, we recursively erase unnecessary vertices and isolated vertices. Isolated vertices refer to the vertices that have neither incoming nor outgoing vertices. Unnecessary vertices refer to the skippable operations, e.g., Concat and Add (between Conv7 and AvgPool) become unnecessary. Ultimately, a compact sub-network \mathcal{M}^* is constructed as shown in Figure 3c. By the definition of GeZIGs, the redundant GeZIGs (have been projected onto zeros) contribute none to the

model outputs. Consequently, the \mathcal{M}^* returns the exact same output as the super-network \mathcal{M} with $\mathbf{x}_{\text{H2SPG}}^*$, which avoids the necessity of further fine-tuning the sub-network.¹

4 Numerical Experiments

In this section, we employ OTOv3 to one-shot automatically train and search within general super-networks to construct compact sub-networks with high performance. The numerical demonstrations cover extensive super-networks including DemoSupNet shown in Section 3, StackedUnets (Ronneberger et al., 2015; Chen et al., 2023), SuperResNet (He et al., 2016; Lin et al., 2021), and DARTS (Liu et al., 2018), and benchmark datasets, including CIFAR10 (Krizhevsky & Hinton, 2009), Fashion-MNIST (Xiao et al., 2017), ImageNet (Deng et al., 2009), STL-10 (Coates et al., 2011) and SVNH (Netzer et al., 2011). More implementation details of experiments and OTOv3 library and limitations are provided in Appendix A. The dependency graphs and the constructed sub-networks are depicted in Appendix E. Ablation studies regarding H2SPG over RegNet (Radosavovic et al., 2020) is present in Appendix C.

Table 1: OTOv3 on extensive super-networks and datasets.

Backend	Dataset	Method	FLOPs (M)	# of Params (M)	Top-1 Acc. (%)
DemoSupNet	Fashion-MNIST	Baseline	209	0.82	84.9
DemoSupNet	Fashion-MNIST	OTOv3	107	0.45	84.7
StackedUnets	SVNH	Baseline	184	0.80	95.3
StackedUnets	SVNH	OTOv3	115	0.37	96.1
DARTS (8 cells)	STL-10	Baseline	614	4.05	74.6
DARTS (8 cells)	STL-10	OTOv3	127	0.64	75.1

DemoSupNet on Fashion-MNIST. We first experiment with the DemoSupNet presented as Figure 1a on Fashion-MNIST. OTOv3 automatically establishes a search space of DemoSupNet and partitions its trainable variables into GeZIGs. H2SPG then trains DemoSupNet from scratch and computes a solution of high performance and hierarchical group-sparsity over GeZIGs, which is further utilized to construct a compact sub-network as presented in Figure 3c. As shown in Table 1, compared to the super-network, the sub-network utilizes 54% of parameters and 51% of FLOPs to achieve a Top-1 validation accuracy 84.7% which is negligibly lower than the super-network by 0.2%.

StackedUnets on SVNH. We then consider a StackedUnets over SVNH. The StackedUnets is constructed by stacking two standard Unets (Ronneberger et al., 2015) with different downsamplers together, as depicted in Figure 6a in Appendix E. We employ OTOv3 to automatically build the dependency graph, establish the search space, and train by H2SPG. H2SPG identifies and projects the redundant structures onto zero and optimize the remaining important ones to attain excellent performance. As displayed in Figure 6c, the right-hand-side Unet is disabled due to node-72-node-73-node-74-node-75 being zero.² The path regarding the deepest depth for the left-hand-side Unet, *i.e.*, node-13-node-14-node-15-node-19, is marked as redundant as well. The results by OTOv3 indicate that the performance gain brought by either composing multiple Unets in parallel or encompassing deeper scaling paths is not significant. OTOv3 also validates the human design since a single Unet with properly selected depths have achieved remarkable success in numerous applications (Ding et al., 2022; Weng et al., 2019). Furthermore, as presented in Table 1, the sub-network built by OTOv3 uses 0.37M parameters and 115M FLOPs which is noticeably lighter than the full StackedUnets meanwhile significantly outperforms it by 0.8% in validation accuracy.

DARTS (8-Cells) on STL-10. We next employ OTOv3 on DARTS over STL-10. DARTS is a complicated super-network consisting of iteratively stacking multiple cells (Liu et al., 2018). Each cell is constructed by spanning a graph wherein every two nodes are connected via multiple operation candidates. STL-10 is an image dataset for the semi-supervising learning, where we conduct the experiments by using its labeled samples. DARTS has been well explored in the recent years. However, the existing NAS methods studied it based on a *handcrafted* search space beforehand to

¹Remark here that the sub-network is still compatible to be fine-tuned afterwards if needed.

²Recall the definition of GeZIG, if one GeZIG equals to zero, its output would be always zero given whatever inputs. Therefore, node-72-node-73-node-74-node-75 only produces zero output even if its ancestor vertices may have non-zero parameters. As a result, the right-hand-side Unet is completely disabled.

locally pick up one or two important operations to connect every two nodes. We now employ OTOv3 on an eight-cells DARTS to *automatically* establish its search space, then utilize H2SPG to one shot train it and search important structures *globally* as depicted in Figure 7c of Appendix E. Afterwards, a sub-network is automatically constructed as drawn in Figure 7d of Appendix E. Quantitatively, the sub-network outperforms the full DARTS in terms of validation accuracy by 0.5% by using only about 15%-20% of the parameters and the FLOPs of the original super-network (see Table 1).

SuperResNet on CIFAR10.

Later on, we switch to a ResNet search space as ZenNAS (Lin et al., 2021), referred to as SuperResNet. SuperResNet is constructed by stacking several super-residual blocks with varying depths. Each super-residual blocks contain multiple Conv candidates with kernel sizes as 3×3, 5×5 and 7×7 separately in parallel (see Figure 8a). We then

employ OTOv3 to one-shot automatically produce two sub-networks with 1M and 2M parameters. As displayed in Table 2, the 1M sub-network by OTOv3 outperforms the counterparts reported in (Lin et al., 2021) in terms of search cost (on an NVIDIA A100 GPU) due to the efficient single-level optimization. The 2M sub-network could reach the benchmark over 97% validation accuracy. Remark here that OTOv3 and ZenNAS use networks of fewer parameters to achieve competitive performance to the DARTS benchmarks. This is because of the extra data-augmentations such as MixUp (Zhang et al., 2017) on this experiment by ZenNAS, so as OTOv3 to follow the same training settings.

Table 2: OTOv3 over SuperResNet on CIFAR10.

Architecture	Top-1 Acc (%)	# of Params (M)	Search Cost (GPU days)
Zen-Score-1M (Lin et al., 2021)	96.2	1.0	0.4
Synflow [†] (Tanaka et al., 2020)	95.1	1.0	0.4
NASWOT [†] (Mellor et al., 2021)	96.0	1.0	0.5
Zen-Score-2M (Lin et al., 2021)	97.5	2.0	0.5
SANAS-DARTS (Hosseini & Xie, 2022)	97.5	3.2	1.2*
ISTA-NAS (He et al., 2020)	97.5	3.3	0.1
CDEP (Rieger et al., 2020)	97.2	3.2	1.3*
DARTS (2nd order) (Liu et al., 2018)	97.2	3.1	1.0
PrDARTS (Zhou et al., 2020)	97.6	3.4	0.2
P-DARTS (Chen et al., 2019)	97.5	3.6	0.3
PC-DARTS (Xu et al., 2019)	97.4	3.9	0.1
OTOv3-SuperResNet-1M	96.3	1.0	0.1
OTOv3-SuperResNet-2M	97.5	2.0	0.1

[†] Reported in (Lin et al., 2021).

* Numbers are approximately scaled based on (Hosseini & Xie, 2022).

Table 3: OTOv3 over DARTS on ImageNet and comparison with state-of-the-art methods.

Architecture	Test Acc. (%)		# of Params (M)	FLOPs (M)	Search Method
	Top-1	Top-5			
Inception-v1 (Szegedy et al., 2015)	69.8	89.9	6.6	1448	Manual
ShuffleNet 2× (v2) (Ma et al., 2018)	74.9	—	5.0	591	Manual
NASNet-A (Zoph et al., 2018)	74.0	91.6	5.3	564	RL
MnasNet-92 (Tan et al., 2019)	74.8	92.0	4.4	388	RL
AmoebaNet-C (Real et al., 2019)	75.7	92.4	6.4	570	Evolution
DARTS (2nd order) (CIFAR10) (Liu et al., 2018)	73.3	91.3	4.7	574	Gradient
P-DARTS (CIFAR10) (Chen et al., 2019)	75.6	92.6	4.9	557	Gradient
PC-DARTS (CIFAR10) (Xu et al., 2019)	74.9	92.2	5.3	586	Gradient
SANAS (CIFAR10) (Hosseini & Xie, 2022)	75.2	91.7	—	—	Gradient
ProxylessNAS (ImageNet) (Cai et al., 2018)	75.1	92.5	7.1	465	Gradient
PC-DARTS (ImageNet) (Xu et al., 2019)	75.8	92.7	5.3	597	Gradient
ISTA-NAS (ImageNet) (Yang et al., 2020)	76.0	92.9	5.7	638	Gradient
OTOv3 on DARTS (ImageNet)	75.3	92.5	4.8	547	Gradient

(CIFAR10) / (ImageNet) refer to using either CIFAR10 or ImageNet for searching architecture.

DARTS (14-Cells) on ImageNet. We finally present the benchmark DARTS super-network stacked by 14 cells on ImageNet. We employ OTOv3 over it to automatically figure out the search space which the code base required specified handcraftness in the past, train by H2SPG to figure out redundant structures, and construct a sub-network as depicted in Figure 9d. Quantitatively, we observe that the sub-network produced by OTOv3 achieves competitive top-1/5 accuracy compared to other state-of-the-arts as presented in Table 3. Remark here that it is *engineeringly* difficult yet to inject architecture variables and build a multi-level optimization upon a search space being automatically constructed and globally searched. The single-level H2SPG does not leverage a validation set as others to favor the architecture search and search over the operations without trainable variables, *e.g.*, skip connection, consequently the achieved accuracy does not outperform PC-DARTS and ISTA-NAS. We leave further accuracy improvement based on the *automatic* search space as future work.

5 Conclusion

We propose the third generation of Only-Train-Once framework (OTOv3). To the best of knowledge, OTOv3 is the first automated system that automatically establishes the search spaces for general

super-networks, then trains the super-networks via a novel H2SPG optimizer in the one-shot manner, finally automatically produces compact sub-networks of high-performance. Meanwhile, H2SPG is also perhaps the first stochastic optimizer that effectively solves a hierarchical structured sparsity problem for deep learning tasks. OTOv3 further significantly reduces the human efforts upon the existing NAS works, opens a new direction and establishes benchmarks regarding the automated NAS for the general super-networks which currently require numerous handcraftness beforehand.

References

- Han Cai, Ligeng Zhu, and Song Han. Proxylessnas: Direct neural architecture search on target task and hardware. *arXiv preprint [arXiv:1812.00332](#)*, 2018.
- Tianyi Chen, Bo Ji, Tianyu Ding, Biyi Fang, Guanyi Wang, Zhihui Zhu, Luming Liang, Yixin Shi, Sheng Yi, and Xiao Tu. Only train once: A one-shot neural network training and pruning framework. In *Advances in Neural Information Processing Systems*, 2021a.
- Tianyi Chen, Luming Liang, DING Tianyu, Zhihui Zhu, and Ilya Zharkov. OTOv2: Automatic, generic, user-friendly. In *The Eleventh International Conference on Learning Representations*, 2023.
- Tianyi Chen, Bo Ji, Yixin Shi, Tianyu Ding, Biyi Fang, Sheng Yi, and Xiao Tu Zharkov. Neural network compression via sparse optimization. In *arXiv preprint [arXiv:2011.04868](#)*, 2020.
- Xin Chen, Lingxi Xie, Jun Wu, and Qi Tian. Progressive differentiable architecture search: Bridging the depth gap between search and evaluation. In *Proceedings of the IEEE/CVF international conference on computer vision*, pp. 1294–1303, 2019.
- Xin Chen, Lingxi Xie, Jun Wu, and Qi Tian. Progressive darts: Bridging the optimization gap for nas in the wild. *International Journal of Computer Vision*, 129:638–655, 2021b.
- Adam Coates, Andrew Ng, and Honglak Lee. An analysis of single-layer networks in unsupervised feature learning. In *Proceedings of the fourteenth international conference on artificial intelligence and statistics*, pp. 215–223. JMLR Workshop and Conference Proceedings, 2011.
- Jia Deng, Wei Dong, Richard Socher, Li-Jia Li, Kai Li, and Li Fei-Fei. Imagenet: A large-scale hierarchical image database. In *2009 IEEE conference on computer vision and pattern recognition*, pp. 248–255. Ieee, 2009.
- Tianyu Ding, Luming Liang, Zhihui Zhu, Tianyi Chen, and Ilya Zharkov. Sparsity-guided network design for frame interpolation. *arXiv preprint [arXiv:2209.04551](#)*, 2022.
- Thomas Elsken, Jan Hendrik Metzen, and Frank Hutter. Efficient multi-objective neural architecture search via lamarckian evolution. *arXiv preprint [arXiv:1804.09081](#)*, 2018.
- Gongfan Fang, Xinyin Ma, Mingli Song, Michael Bi Mi, and Xinchao Wang. Depgraph: Towards any structural pruning. *arXiv preprint [arXiv:2301.12900](#)*, 2023.
- Ian Goodfellow, Yoshua Bengio, Aaron Courville, and Yoshua Bengio. *Deep learning*, volume 1. MIT press Cambridge, 2016.
- Song Han, Huizi Mao, and William J Dally. Deep compression: Compressing deep neural networks with pruning, trained quantization and huffman coding. *arXiv preprint [arXiv:1510.00149](#)*, 2015.
- Chaoyang He, Haishan Ye, Li Shen, and Tong Zhang. Milenas: Efficient neural architecture search via mixed-level reformulation. In *Proceedings of the IEEE/CVF Conference on Computer Vision and Pattern Recognition*, pp. 11993–12002, 2020.
- Kaiming He, Xiangyu Zhang, Shaoqing Ren, and Jian Sun. Deep residual learning for image recognition. In *Proceedings of the IEEE conference on computer vision and pattern recognition*, 2016.
- Ramtin Hosseini and Pengtao Xie. Saliency-aware neural architecture search. *Advances in Neural Information Processing Systems*, 35:14743–14757, 2022.

- Ilija Radosavovic, Raj Prateek Kosaraju, Ross Girshick, Kaiming He, and Piotr Dollár. Designing network design spaces. *Proceedings of the IEEE/CVF conference on computer vision and pattern recognition*, 2020.
- Diederik P Kingma and Jimmy Ba. Adam: A method for stochastic optimization. *arXiv preprint arXiv:1412.6980*, 2014.
- A. Krizhevsky and G. Hinton. Learning multiple layers of features from tiny images. *Master’s thesis, Department of Computer Science, University of Toronto*, 2009.
- Yann LeCun, Yoshua Bengio, and Geoffrey Hinton. Deep learning. *nature*, 521(7553):436–444, 2015.
- Ming Lin, Pichao Wang, Zhenhong Sun, Heseng Chen, Xiuyu Sun, Qi Qian, Hao Li, and Rong Jin. Zen-nas: A zero-shot nas for high-performance deep image recognition. In *2021 IEEE/CVF International Conference on Computer Vision, ICCV 2021*, 2021.
- Shaohui Lin, Rongrong Ji, Yuchao Li, Cheng Deng, and Xuelong Li. Toward compact convnets via structure-sparsity regularized filter pruning. *IEEE transactions on neural networks and learning systems*, 31(2):574–588, 2019.
- Hanxiao Liu, Karen Simonyan, and Yiming Yang. Darts: Differentiable architecture search. *arXiv preprint arXiv:1806.09055*, 2018.
- Ningning Ma, Xiangyu Zhang, Hai-Tao Zheng, and Jian Sun. Shufflenet v2: Practical guidelines for efficient cnn architecture design. In *Proceedings of the European conference on computer vision (ECCV)*, pp. 116–131, 2018.
- Joe Mellor, Jack Turner, Amos Storkey, and Elliot J Crowley. Neural architecture search without training. In *International Conference on Machine Learning*, pp. 7588–7598. PMLR, 2021.
- Yuval Netzer, Tao Wang, Adam Coates, Alessandro Bissacco, Bo Wu, and Andrew Y Ng. Reading digits in natural images with unsupervised feature learning. 2011.
- Hieu Pham, Melody Guan, Barret Zoph, Quoc Le, and Jeff Dean. Efficient neural architecture search via parameters sharing. In *International conference on machine learning*, pp. 4095–4104. PMLR, 2018.
- Esteban Real, Alok Aggarwal, Yanping Huang, and Quoc V Le. Regularized evolution for image classifier architecture search. In *Proceedings of the aaai conference on artificial intelligence*, volume 33, pp. 4780–4789, 2019.
- Laura Rieger, Chandan Singh, William Murdoch, and Bin Yu. Interpretations are useful: penalizing explanations to align neural networks with prior knowledge. In *International conference on machine learning*, pp. 8116–8126. PMLR, 2020.
- Olaf Ronneberger, Philipp Fischer, and Thomas Brox. U-net: Convolutional networks for biomedical image segmentation. In *International Conference on Medical image computing and computer-assisted intervention*, pp. 234–241. Springer, 2015.
- Christian Szegedy, Wei Liu, Yangqing Jia, Pierre Sermanet, Scott Reed, Dragomir Anguelov, Dumitru Erhan, Vincent Vanhoucke, and Andrew Rabinovich. Going deeper with convolutions. In *Proceedings of the IEEE conference on computer vision and pattern recognition*, pp. 1–9, 2015.
- Mingxing Tan, Bo Chen, Ruoming Pang, Vijay Vasudevan, Mark Sandler, Andrew Howard, and Quoc V Le. Mnasnet: Platform-aware neural architecture search for mobile. In *Proceedings of the IEEE/CVF conference on computer vision and pattern recognition*, pp. 2820–2828, 2019.
- Hidehiko Tanaka, Daniel Kunin, Daniel L Yamins, and Surya Ganguli. Pruning neural networks without any data by iteratively conserving synaptic flow. *Advances in neural information processing systems*, 33:6377–6389, 2020.

- Ashish Vaswani, Noam Shazeer, Niki Parmar, Jakob Uszkoreit, Llion Jones, Aidan N Gomez, Lukasz Kaiser, and Illia Polosukhin. Attention is all you need. In I. Guyon, U. V. Luxburg, S. Bengio, H. Wallach, R. Fergus, S. Vishwanathan, and R. Garnett (eds.), *Advances in Neural Information Processing Systems*, volume 30. Curran Associates, Inc., 2017.
- Yu Weng, Tianbao Zhou, Yujie Li, and Xiaoyu Qiu. Nas-unet: Neural architecture search for medical image segmentation. *IEEE access*, 7:44247–44257, 2019.
- Han Xiao, Kashif Rasul, and Roland Vollgraf. Fashion-mnist: a novel image dataset for benchmarking machine learning algorithms, 2017.
- Lin Xiao and Tong Zhang. A proximal stochastic gradient method with progressive variance reduction. *SIAM Journal on Optimization*, 24(4):2057–2075, 2014.
- Yuhui Xu, Lingxi Xie, Xiaopeng Zhang, Xin Chen, Guo-Jun Qi, Qi Tian, and Hongkai Xiong. Pc-darts: Partial channel connections for memory-efficient architecture search. *arXiv preprint arXiv:1907.05737*, 2019.
- Yibo Yang, Hongyang Li, Shan You, Fei Wang, Chen Qian, and Zhouchen Lin. Ista-nas: Efficient and consistent neural architecture search by sparse coding. *Advances in Neural Information Processing Systems*, 33:10503–10513, 2020.
- Yutong Dai, Tianyi Chen, Guanyi Wang, and Daniel Robinson. An Adaptive Half-Space Projection Method for Stochastic Optimization Problems with Group Sparse Regularization. In *Transactions on Machine Learning Research*, 2023.
- Hongyi Zhang, Moustapha Cisse, Yann N Dauphin, and David Lopez-Paz. mixup: Beyond empirical risk minimization. *arXiv preprint arXiv:1710.09412*, 2017.
- Peng Zhao, Guilherme Rocha, and Bin Yu. The composite absolute penalties family for grouped and hierarchical variable selection. 2009.
- Pan Zhou, Caiming Xiong, Richard Socher, and Steven Chu Hong Hoi. Theory-inspired path-regularized differential network architecture search. *Advances in Neural Information Processing Systems*, 33:8296–8307, 2020.
- Barret Zoph and Quoc V Le. Neural architecture search with reinforcement learning. *arXiv preprint arXiv:1611.01578*, 2016.
- Barret Zoph, Vijay Vasudevan, Jonathon Shlens, and Quoc V Le. Learning transferable architectures for scalable image recognition. In *Proceedings of the IEEE conference on computer vision and pattern recognition*, pp. 8697–8710, 2018.

A Implementation Details

We provide more implementation details of OTOv3 library and experiments. The official version along with documentations and tutorials will be released to the public after the review process.

A.1 Library Implementations

Overview. OTOv3 is built upon the OTOv2 library that enables automatic general sup-network training and searching sub-networks in the one-shot manner. Up to the present, the implementation of OTOv3 depends on PyTorch and ONNX (<https://onnx.ai>). ONNX is used to obtain the trace graph and the sub-network by modifying the super-network in ONNX format. H2SPG is developed as an instance of the PyTorch optimizer class. As a fundamental AI infrastructure, OTOv3 makes a significant breakthrough in AutoML to first enable the search of sub-networks from training general super-networks. Further progress and contributions from both our team and the wider open-source community are necessary to sustain its continued success.

Limitations. The current version of the library relies on ONNX, which means that the super-networks need to be convertible into the ONNX format. Meanwhile, if the super-network contains unsupported operators, the library may not function normally. To address this, we are committed to maintaining and adding new operators to the library, and leverage contributions from the open-source community in this regard. Additionally, we are actively working on reducing the dependency on ONNX to broaden the library’s coverage and compatibility.

Furthermore, to prioritize generality, we avoid requiring users to manually introduce auxiliary architecture variables, as seen in the existing gradient-based NAS methods. To search without architecture variables, the current OTOv3 library formulates a hierarchical structured sparsity optimization to identify redundant minimal removal structures based on sparse optimization. We currently require the minimal removal structures to have trainable variables. Consequently, the operations without trainable variables such as `skip connection` are not removal for the current version of OTOv3 yet. Identifying and removing operations without trainable variables is an aspect that we consider as future work and plan to address in subsequent updates.

A.2 Experiment Implementations

All experiments were conducted on an NVIDIA A100 GPU. The search cost of OTOv3 was calculated as the runtime of the warm-up phase in Algorithm 3, since it is during this phase that the redundant group candidates are constructed. In our experiments, H2SPG follows the existing NAS works (Liu et al., 2018) by performing 50 epochs for architecture search during the warm-up phase and evolving the learning rate using a cosine annealing scheduler.

For the SuperResNet experiments, we adopt the data augmentation technique of MixUp, following the training settings of ZenNAS (Lin et al., 2021), and employ a multiple-period cosine annealing scheduler. The maximum number of epochs for the DemoSupNet and StackedUnets is set to 300 following (Chen et al., 2023). In the case of DARTS on ImageNet, we expedite the training process by constructing a sub-network once the desired redundant group sparsity level is reached. We then train this sub-network until convergence. All other experiments are carried out in the one-shot manner.

The initial learning rate is set to 0.1 for most experiments, except for the DARTS experiments where it is set to 0.01. The lower initial learning rate in DARTS is due to the absence of auxiliary architecture variables in our super-network, which compute a weighted sum of outputs. Additionally, operations without trainable variables, such as `skip connections`, are preserved (refer to the limitations). Consequently, the cosine annealing period is repeated twice for the DARTS experiments to account for the smaller initial learning rate. The mini-batch sizes are selected as 64 for all tested datasets, except for ImageNet, where it is set to 128. The target group sparsities are estimated in order to achieve a comparable number of parameters to other benchmarks. This is accomplished by randomly selecting a subset of GeZIGs to be zero and then calculating the parameter quantities in the constructed sub-networks. The remaining hyper-parameter settings of H2SPG adhere to the default settings of DHSPG in OTOv2.

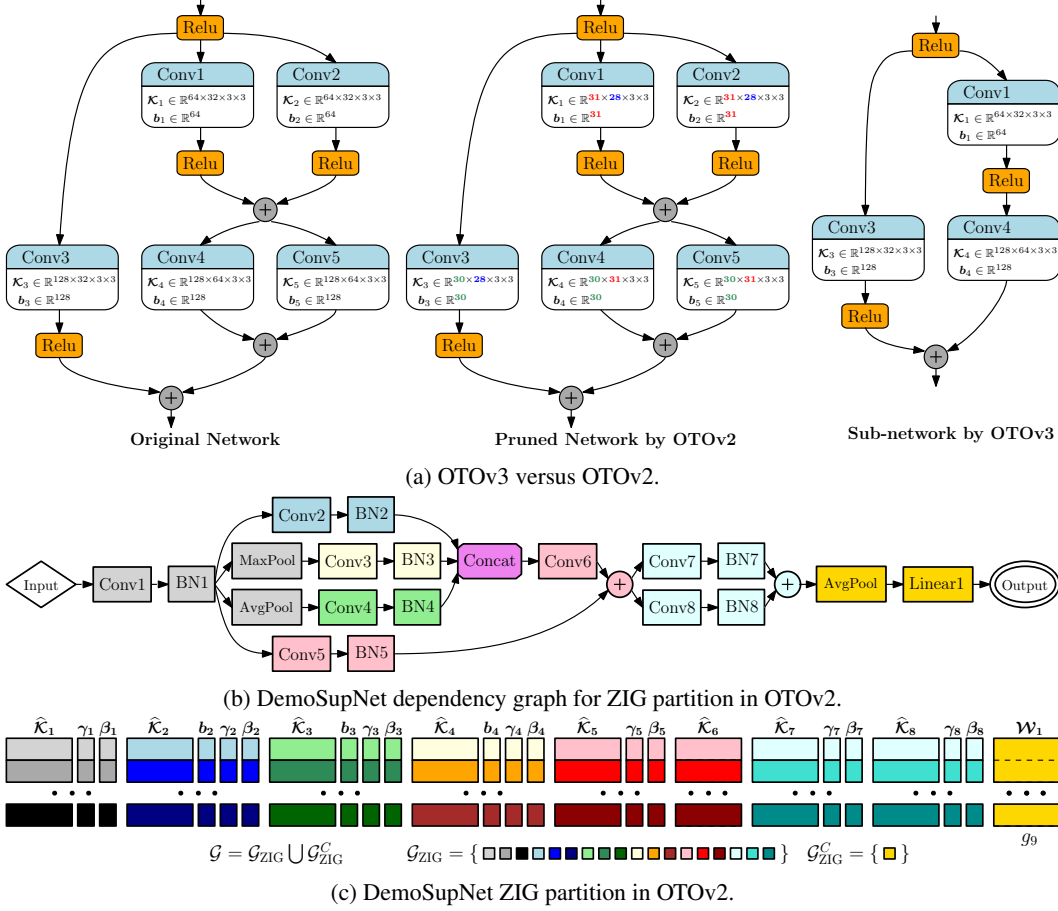


Figure 4: (a) OTOv3 versus OTOv2. (b) Dependency graph for DemoSupNet by OTOv2 for automatic structured pruning. (c) ZIG partition for DemoSupNet by OTOv2.

B ZIG versus GeZIG

We aim to clarify the distinction between the Zero-Invariant Group (ZIG) introduced in OTOv2 (Chen et al., 2023) and the Generalized Zero-Invariant Group (GeZIG) proposed in this work. Broadly speaking, ZIG and GeZIG refer to different categories of minimal removal structures satisfying zero-invariant property, serving distinct purposes to search optimal architecture within the super-network.

A minimal removal structure refers to a structure that satisfies two conditions: (i) removing it from the deep neural network (DNN) still leaves a valid network, and (ii) the structure cannot be further decomposed into smaller removal structures, making it minimal. The specific forms of minimal removal structures depend on whether the vertices (representing operations) and edges (representing connections) in the trace graph are preserved or not.

ZIG (Zero-Invariant Group) pertains to the minimal removal structure employed in the context of structure pruning. In structure pruning, the vertices (operations) and edges (connections) of the trace graph $(\mathcal{V}, \mathcal{E})$ are preserved, but the vertices become slimmer. In contrast, GeZIG (Generalized Zero-Invariant Group) focuses on the standard NAS³ problem that involves removing redundant vertices and edges entirely. GeZIG considers the entire removal of vertices and edges in order to search for more compact and efficient network architectures.

Figure 4a presents the difference between OTOv3 and OTOv2, which train the super-networks and search compact sub-networks from different perspectives. Consequently, the dependency graph for the GeZIG partition differs significantly from the dependency graph for the ZIG partition.

³Structured pruning actually can be interpreted as NAS as well, *i.e.*, searching inside each operation.

As illustrated Figure 4b, which shows the example of dependency graph for ZIG over DemoSupNet, the connected components marked with the same color represent vertices that have affiliations and need to be pruned together. For instance, the output tensors of Conv5-BN5 and Conv6 are added together, requiring them to have the same shapes for the addition operation. Therefore, both Conv5-BN5 and Conv6 need to be slimmed by removing the same number of filters, bias or weight scalars. Consequently, their filters, bias scalar, BN bias, and weight bias are grouped together as a single ZIG, as depicted in Figure 4c.

In contrast, GeZIG groups the trainable variables of several entire vertices together, as shown in Figure 1c. Moreover, GeZIG needs to consider the hierarchy of the dependency graph to ensure the validity of the sub-network since entire connections and vertices are removed. This hierarchical consideration is necessary for NAS and brings significant challenges to the structured sparse optimizers.

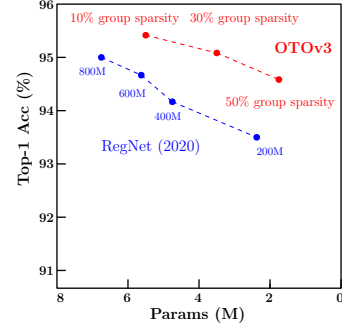
C Ablation Studies

In this appendix, we conduct extensive experiments and ablation studies over one more benchmark architecture RegNet (Radosavovic et al., 2020) on CIFAR10. Without loss of generality, we employ OTov3 over the RegNet-800M which has accuracy 95.01% on CIFAR10 according to <https://github.com/yhhhli/RegNet-Pytorch>. As other experiments, OTov3 automatically constructs its search space, trains via H2SPG, and establishes the sub-networks without fine-tuning.

We conduct ablations by employing OTov3 with two sparse optimizers: H2SPG and DHSPG. We separately evaluate them with varying target hierarchical group sparsity levels in problem (1) across a range of $\{0.1, 0.3, 0.5, 0.7, 0.9\}$. The obtained results are from three independent tests initialized with different random seeds, and reported in Table 4.

Table 4: OTov3 on RegNet on CIFAR10.

Backend	Method	Optimizer	Target Group Sparsity	# of Params (M)	Top-1 Acc. (%)
RegNet-200M	Baseline	SGD	—	2.31	93.58
RegNet-400M	Baseline	SGD	—	4.77	94.15
RegNet-600M	Baseline	SGD	—	5.67	94.73
RegNet-800M	Baseline	SGD	—	6.60	95.01
RegNet-800M	OTov3	DHSPG	0.1	5.56 ± 0.02	95.26 ± 0.13
RegNet-800M	OTov3	DHSPG	0.3	$(3.40, \mathbf{X}, \mathbf{X})$	$(95.01, \mathbf{X}, \mathbf{X})$
RegNet-800M	OTov3	DHSPG	0.5	$(\mathbf{X}, \mathbf{X}, \mathbf{X})$	$(\mathbf{X}, \mathbf{X}, \mathbf{X})$
RegNet-800M	OTov3	DHSPG	0.7	$(\mathbf{X}, \mathbf{X}, \mathbf{X})$	$(\mathbf{X}, \mathbf{X}, \mathbf{X})$
RegNet-800M	OTov3	DHSPG	0.9	$(\mathbf{X}, \mathbf{X}, \mathbf{X})$	$(\mathbf{X}, \mathbf{X}, \mathbf{X})$
RegNet-800M	OTov3	H2SPG	0.1	5.58 ± 0.01	95.30 ± 0.10
RegNet-800M	OTov3	H2SPG	0.3	3.54 ± 0.15	95.08 ± 0.14
RegNet-800M	OTov3	H2SPG	0.5	1.83 ± 0.09	94.61 ± 0.19
RegNet-800M	OTov3	H2SPG	0.7	1.16 ± 0.12	91.92 ± 0.24
RegNet-800M	OTov3	H2SPG	0.9	0.82 ± 0.17	87.91 ± 0.32



Sub-networks by OTov3 versus Super-Networks. As presented in Table 4, the sub-networks under varying hierarchical group sparsity levels computed by OTov3 with H2SPG exhibits the Pareto frontier comparing with the benchmark RegNet. Notably, the sub-networks under target group sparsity levels of 0.1 and 0.3 outperform the full RegNet-800M. Furthermore, the sub-network produced with a group sparsity level of 0.5 outperforms the RegNet200M, RegNet400M, and RegNet600M, despite utilizing significantly fewer parameters while achieving higher accuracy.

H2SPG versus DHSPG. In Table 4, a comparison between H2SPG and DHSPG reveals that DHSPG often fails when confronts with reasonably large target sparsity levels. The failure tests are denoted by the symbol \mathbf{X} . The underlying reason lies in its design, which solely treats problem (1) as an independent and disjoint structured sparsity problem. By disregarding the hierarchy within the network, DHSPG easily generates sub-networks that lack validity. Conversely, H2SPG takes into account the network hierarchy and successfully addresses the target problem (1). This stark contrast highlights the superior performance of H2SPG in producing valid sub-networks via identifying and removing entire redundant operations and connections.

D Complexity Analysis

We end the appendix via analyzing the time and space complexity in OTov3 to construct the search space and the hierarchy consideration during H2SPG optimization.

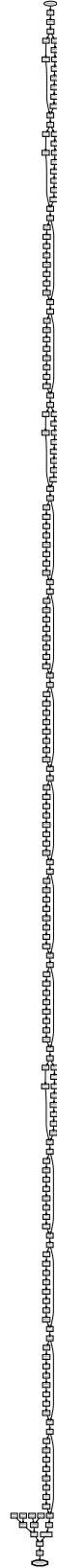
Search Space Construction. The automatic search space construction Algorithm 2 primarily a customized graph algorithm designed to identify minimal removal structures and partition trainable variables into GeZIGs. It contains two main stages: (i) establishing the dependency graph, and (ii) constructing the GeZIG partition. During the first stage, the algorithm traverses the trace graph using a combination of depth-first and breadth-first approaches with specific operations. Consequently, the worst-case time complexity is $\mathcal{O}(|\mathcal{V}| + |\mathcal{E}|)$ to visit every vertex and edge in the trace graph. The worst-case space complexity equals to $\mathcal{O}(|\mathcal{V}|)$ due to the queue container used in Algorithm 2 and the cache employed during the recursive depth-first search. In the second stage, the constructed dependency graph $(\mathcal{V}_d, \mathcal{E}_d)$ is traversed in a depth-first manner to perform the GeZIG partition. In the worst case scenario, where $(\mathcal{V}_d, \mathcal{E}_d)$ equals $(\mathcal{V}, \mathcal{E})$, the time and space complexities remain the same as $\mathcal{O}(|\mathcal{V}| + |\mathcal{E}|)$ and $\mathcal{O}(|\mathcal{V}|)$ respectively. In summary, the worst-case time complexity for both stages combined is $\mathcal{O}(|\mathcal{V}| + |\mathcal{E}|)$, and the worst-case space complexity is $\mathcal{O}(|\mathcal{V}|)$. Therefore, the search space construction can be typically efficiently finished in practice.

Hierarchy Structured Sparsity Optimization. Compared to standard structured sparsity optimizers, H2SPG takes into account of the hierarchy of the network during optimization to ensure the validity of the generated sub-networks. This is achieved through a hierarchy check, which involves removing one vertex from the dependency graph $(\mathcal{V}_d, \mathcal{E}_d)$ and determining if the remaining DNN remains connected from the input to the output. A depth-first search is performed for this purpose, with a worst-case time complexity of $\mathcal{O}(|\mathcal{V}_d| + |\mathcal{E}_d|)$ and a worst-case space complexity of $\mathcal{O}(|\mathcal{V}_d|)$.

Throughout the optimization process, the hierarchy check is only triggered once iteratively over a subset of minimal removal structures (proportional to the target group sparsity level). This check occurs immediately after the warm-up phase in Algorithm 3. Consequently, the worst-case overall time complexity for the hierarchy check is $\mathcal{O}(|\mathcal{V}_d|^2 + |\mathcal{E}_d| \cdot |\mathcal{V}_d|)$. The worst-case overall space complexity remains $\mathcal{O}(|\mathcal{V}_d|)$, since the cache used for the hierarchy check is cleaned up after each vertex completes its own check. Remark here that although the worst-case time complexity is quadratic in the number of vertices of the constructed dependency graph, the hierarchy check can be *efficiently* executed in practice because the number of vertices in the dependency graph is typically reasonably limited. Additionally, the hierarchy check only occurs *once* during the entire optimization process, consequently does not bring significant computational overhead to the whole process.

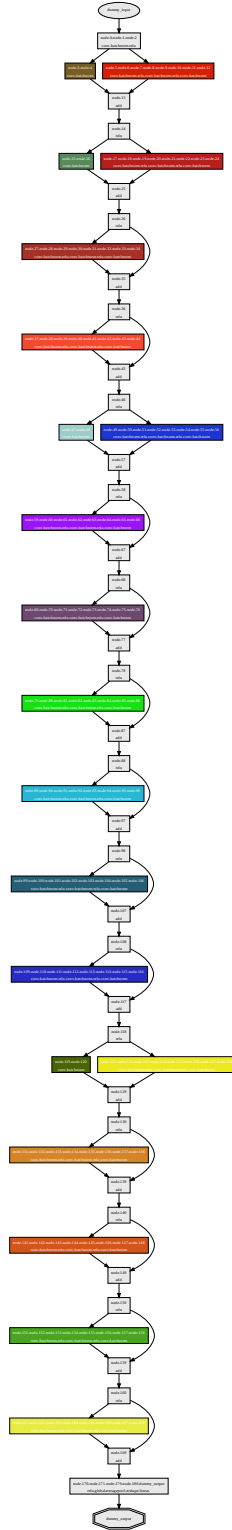
E Graph Visualizations

In this appendix, we present visualizations generated by the OTov3 library to provide more intuitive illustrations of the architectures tested in the paper. The visualizations include trace graphs, dependency graphs, identified redundant GeZIGs, and constructed sub-networks. To ensure clear visibility, we highly recommend **zooming in with an upscale ratio of at least 500%** to observe finer details and gain a better understanding of the proposed system.



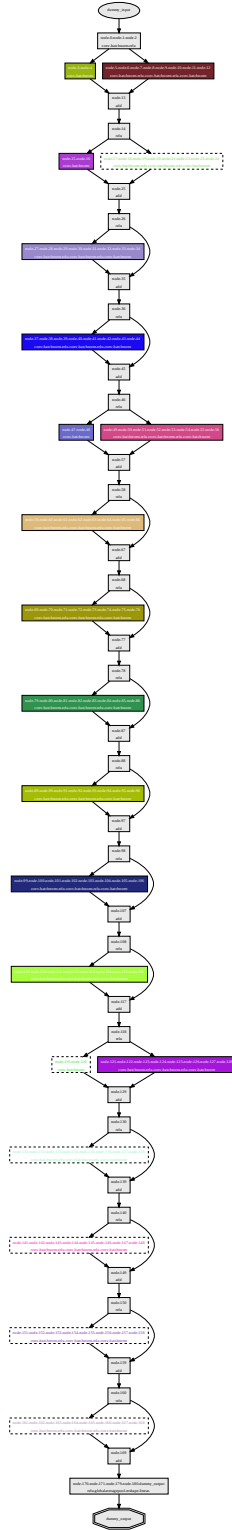
(a) RegNet trace graph.

Figure 5: RegNet illustrations drawn by OTov3.



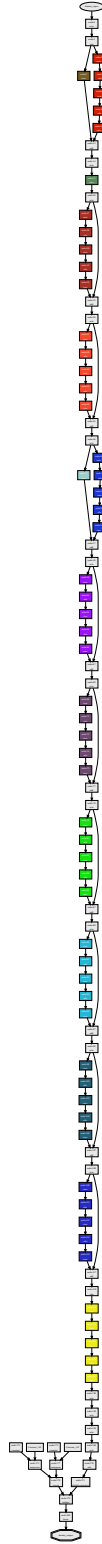
(b) RegNet search space.

Figure 5: RegNet illustrations drawn by OTov3.



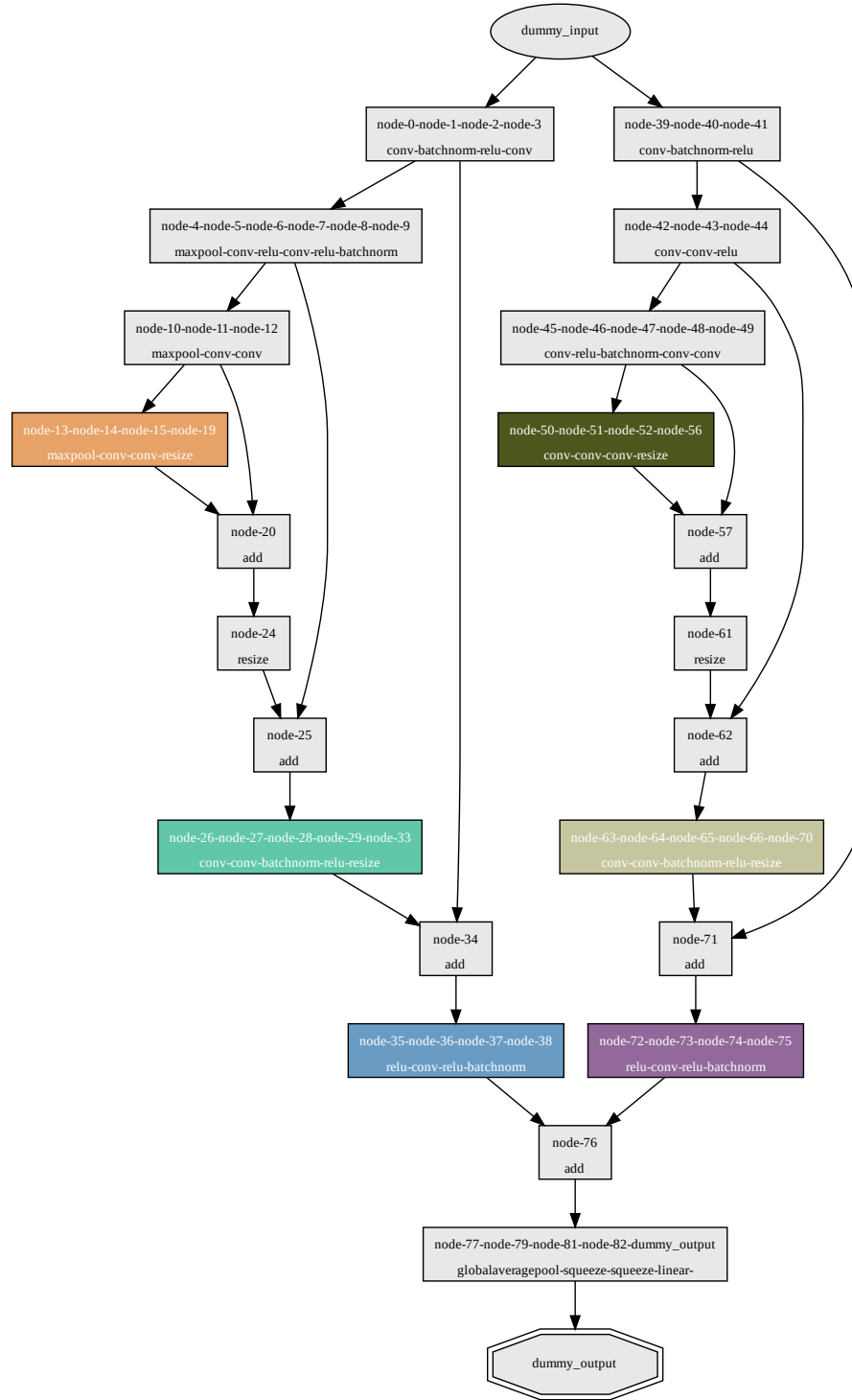
(c) RegNet dependency graph with identified removal vertices.

Figure 5: RegNet illustrations drawn by OTov3.



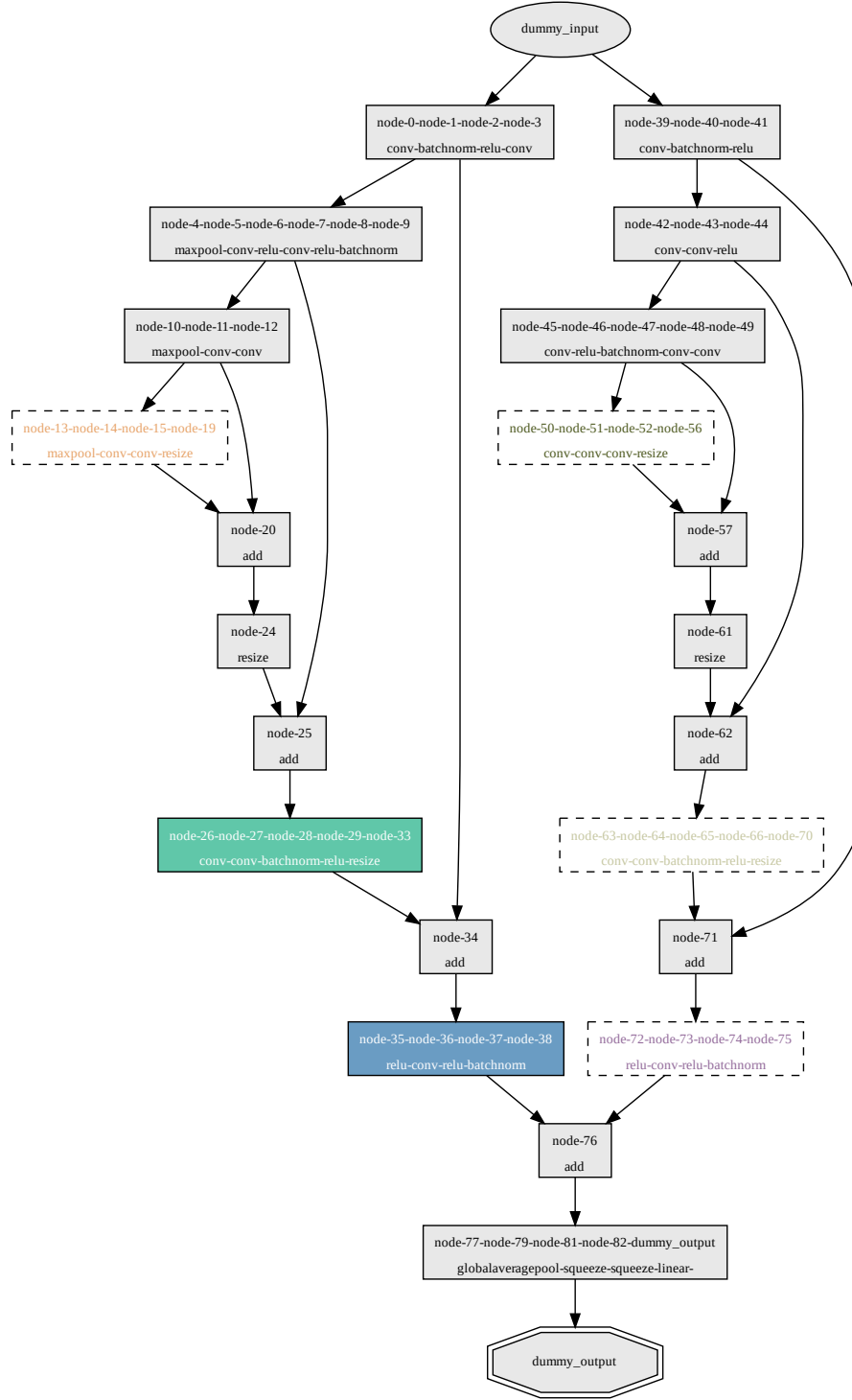
(d) Constructed sub-network upon RegNet.

Figure 5: RegNet illustrations drawn by OTOv3.



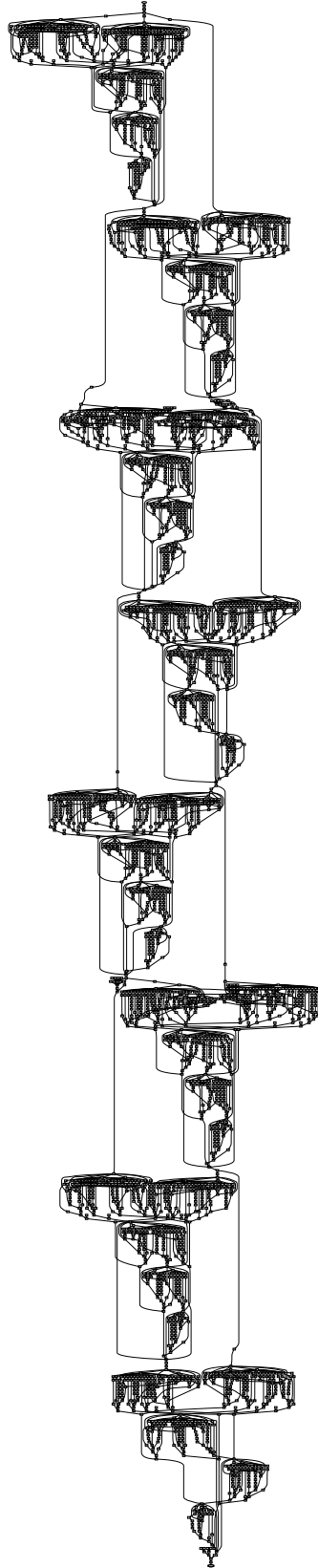
(b) StackedUnets search space.

Figure 6: StackedUnets illustrations drawn by OTOv3.



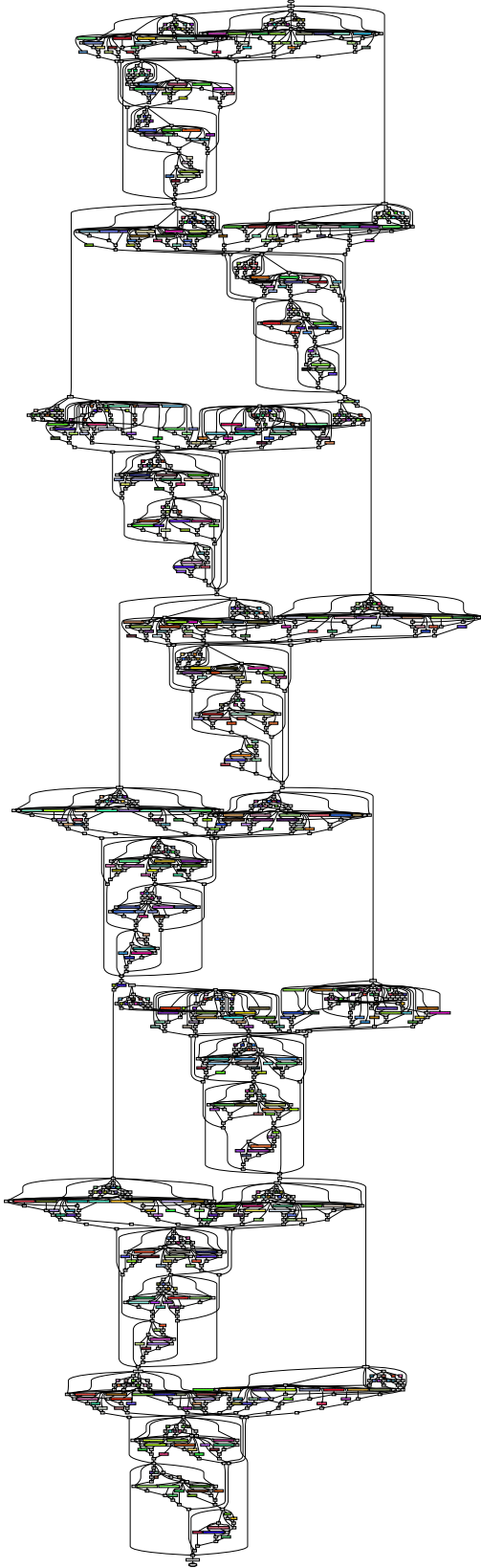
(c) StackedUnets dependency graph with identified removal vertices.

Figure 6: StackedUnets illustrations drawn by OTOv3.



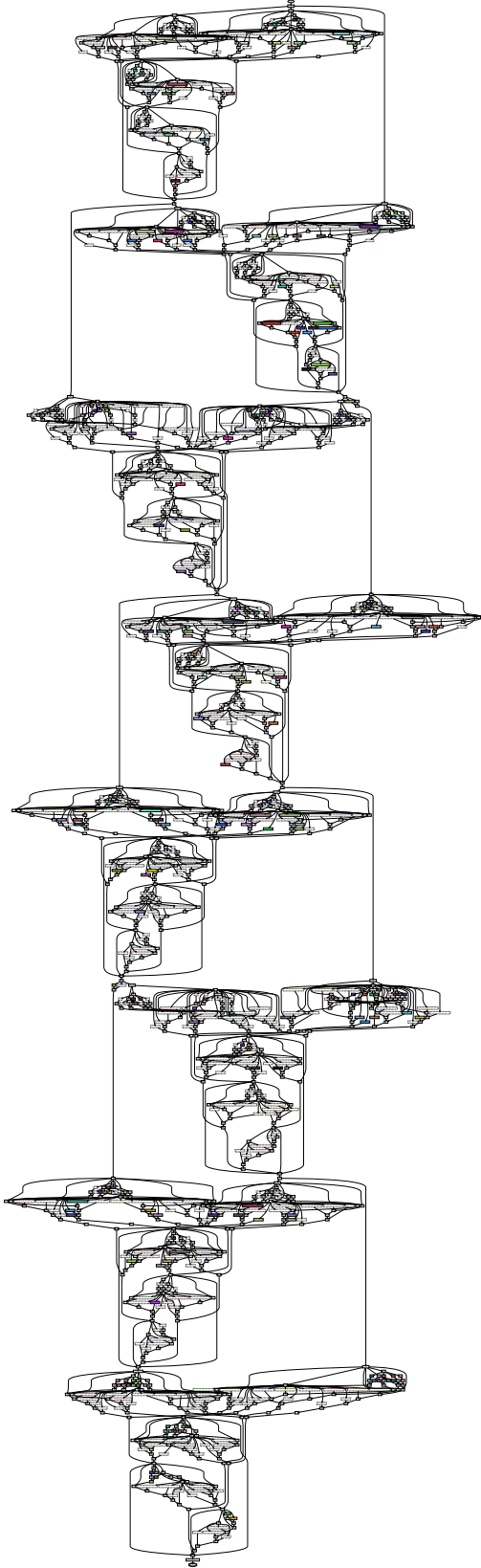
(a) DARTS (8 cells) trace graph.

Figure 7: DARTS (8 cells) illustrations drawn by OTov3.



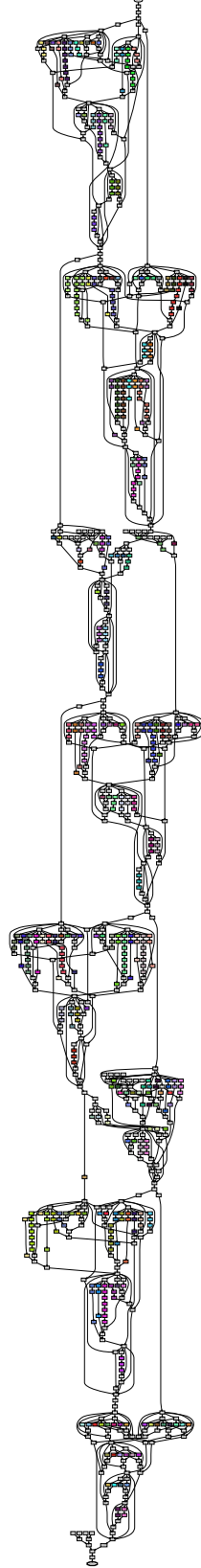
(b) DARTS (8 cells) search space.

Figure 7: DARTS (8 cells) illustrations drawn by OTov3.



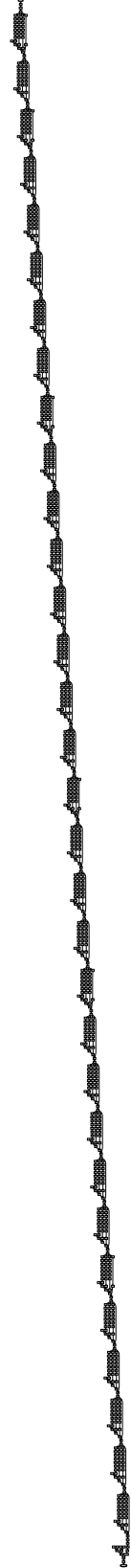
(c) DARTS (8 cells) dependency graph with identified removal vertices.

Figure 7: DARTS (8 cells) illustrations drawn by OTov3.



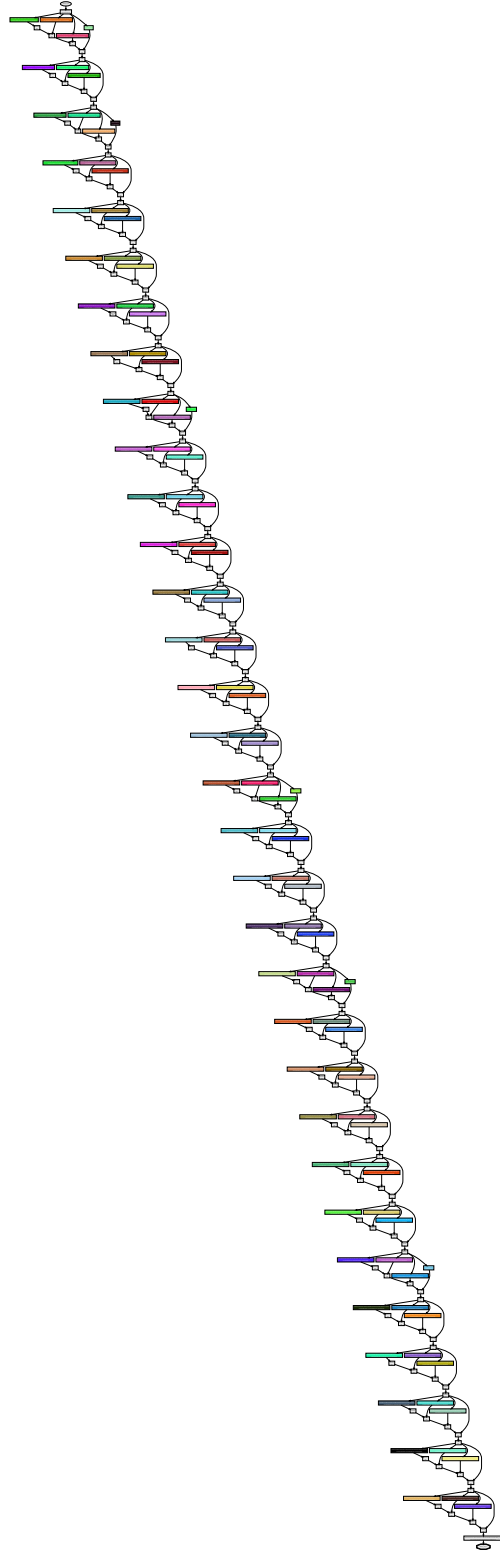
(d) Constructed sub-network upon DARTS (8 cells).

Figure 7: DARTS (8 cells) illustrations drawn by OTov3.



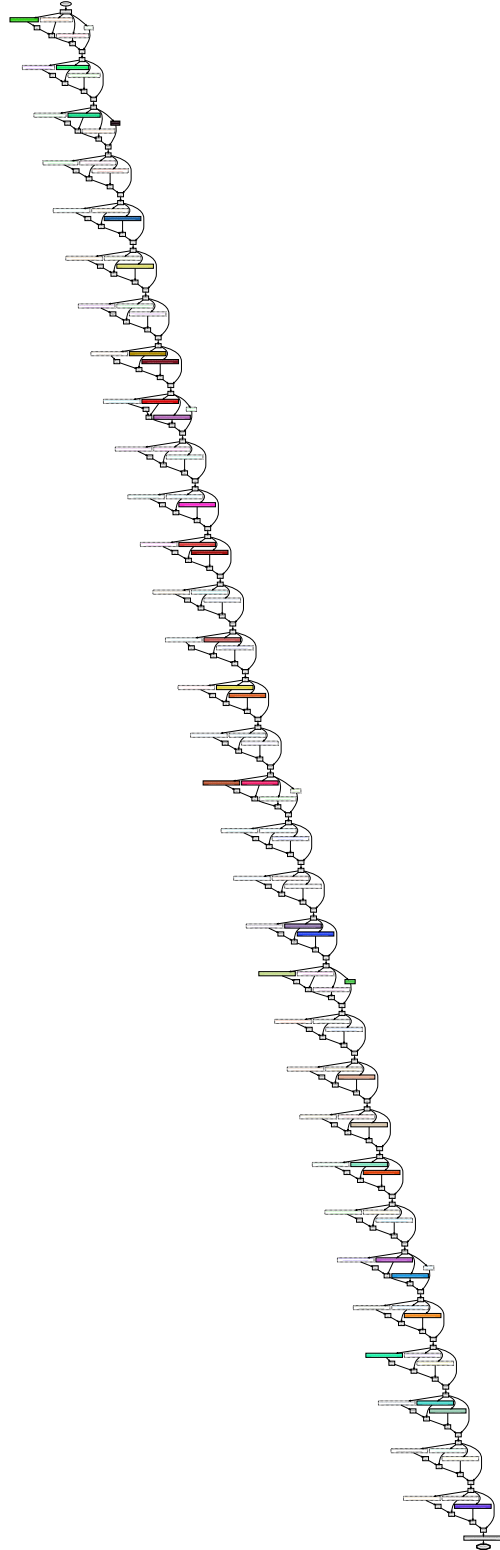
(a) SuperResNet trace graph.

Figure 8: SuperResNet illustrations drawn by OTOv3.



(b) SuperResNet search space.

Figure 8: SuperResNet illustrations drawn by OTov3.



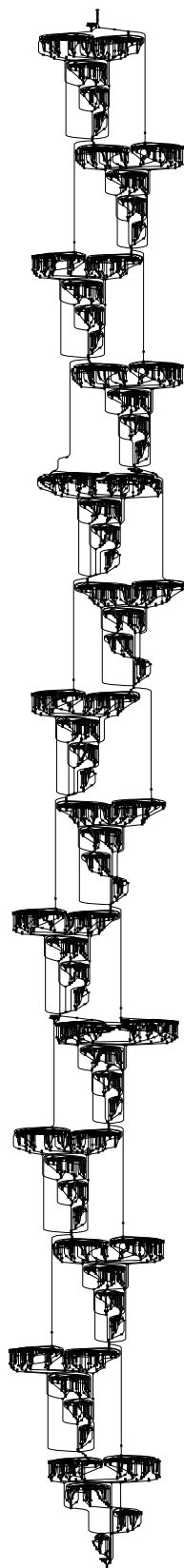
(c) SuperResNet dependency graph with identified removal vertices.

Figure 8: SuperResNet illustrations drawn by OTov3.



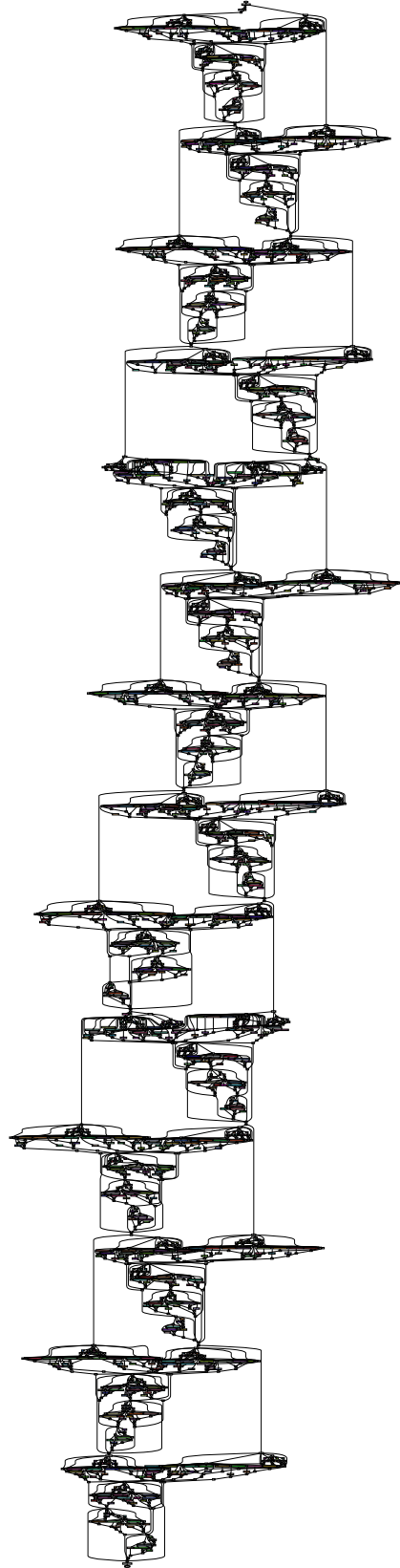
(d) Constructed sub-network upon SuperResNet.

Figure 8: SuperResNet illustrations drawn by OTov3.



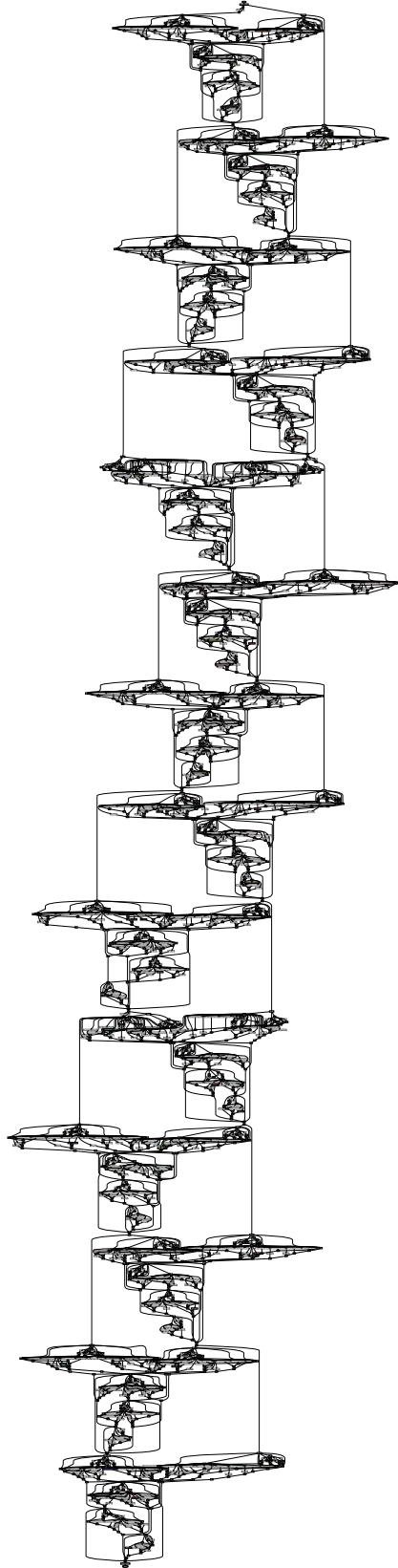
(a) DARTS (14 cells) trace graph.

Figure 9: DARTS (14 cells) illustrations drawn by OTov3.



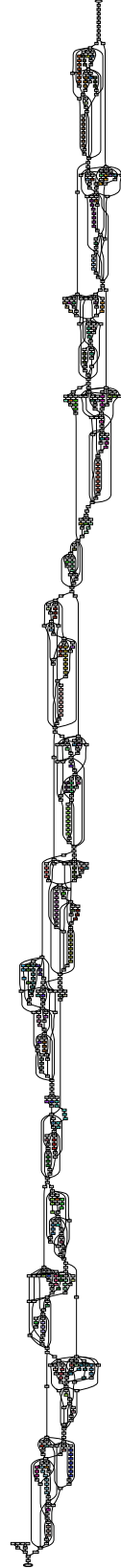
(b) DARTS (14 cells) search space.

Figure 9: DARTS (14 cells) illustrations drawn by OTov3.



(c) DARTS (14 cells) dependency graph with identified removal vertices.

Figure 9: DARTS (14 cells) illustrations drawn by OTov3.



(d) Constructed sub-network upon DARTS (14 cells).

Figure 9: DARTS (14 cells) illustrations drawn by OTov3.